Journal of Materials and Electronic Devices 1(2016) 40-44

JOURNAL OF MATERIALS AND ELECTRONICS

Publishing Company

http://dergi.firat.edu.tr/index.php/jmed

Analysis of the current-voltage (I-V) characteristics of MIS device as a function of gamma irradiation

Adem Tataroğlu

Department of Physics, Faculty of Sciences, Gazi University, 06500, Ankara, Turkey

The effects of gamma radiation on the current-voltage (I-V) characteristics of Au/Si_3N_4/n-Si (MIS) device were investigated, and the radiation effects discussed in detail. The MIS device was exposed to different irradiation doses, ranging from 0 to 100 kGy. The reverse and forward bias I-V curves showed a decrease in current with the increasing radiation dose. The values of ideality factor (n), barrier height (Φ_{B0}) and the reverse saturation current (I_o) for each irradiation dose were obtained from the forward bias I-V characteristics. The ideality factor and saturation current decreases, while the barrier height increases with increase in the radiation dose. Moreover, the value of series resistance (R_S) calculated from Cheung's functions increases with increase in the radiation dose.

Keywords: Gamma-ray; MIS device; Ideality factor; Barrier height; Series resistance

Submission date:12 November 2015

Acceptance date:1 January 2016

Corresponding authors: ademta71@gmail.com (A. Tataroğlu)

1. Introduction

Semiconductor-based devices such as metal-semiconductor (MS), metal-insulator-semiconductor (MIS) and metal-oxide-semiconductor (MOS) play a decisive role in the semiconductor industry. The insulator layer so-called oxide film such as SiO_2, SnO_2, TiO_2 and Si_3N_4 is an important part of the MIS and MOS devices. The insulator layer not only prevents the reaction and interdiffusion between metal and semiconductor, but also alleviates the electric field reduction issue of these devices. The reliability and performance of MIS and MOS devices depend mainly on the formation of insulator/oxide layer grown on the semiconductor, the density of interface states (N_{ss}) and series resistance (R_s). Moreover, the electrical characteristics of these devices are strongly dependent on applied voltage, frequency, temperature and exposure to ionizing radiation [1-8].

Radiation is very important for the long-term reliability of MIS and MOS device, and it can affect device performance and electrical characteristics. Radiation consists of high energy particles such as neutrons, protons and electrons, and energetic gamma-ray and x-ray photons. If the semiconductor device exposures to these radiations, electron-hole pairs can be created in the device [1,9-12]. The electron-hole pairs are produced as the incident charged particle loses energy to electrons bound to the lattice. Although some of the radiation-generated electron-hole pairs in the oxide recombine. Radiation-generated holes become trapped in the oxide for positive gate bias, and then they transport to the oxide/semiconductor interface. The radiation-induced interface traps at the oxide-semiconductor interface are localized states with energy levels in semiconductor band-gap, and they lead to the formation of interface states. The interface states can change the electrical characteristics of the irradiated device [1,13-15].

The purpose of this work is to investigate the effects of gamma radiation on the current-voltage (I-V) characteristics of the fabricated MIS device. The electrical parameters of the MIS device are extracted from the forward bias I-V measurements before and after gamma irradiation.

2. Experimental details

Au/Si_3N_4/n-Si (MIS) device was fabricated on phosphorus doped (n-type) single crystal Si substrate with a 2" diameter, 300μm thickness, (100) orientation, and 0.5 Ω.cm resistivity. Before the fabrication process, the substrate was chemically cleaned using the conventional method and then chemically etched and finally quenched in deionized water. After cleaning and etching steps, the substrate was mounted on a stainless steel sputtering holder that was heated optically and loaded into a radio frequency magnetron sputtering system. The Si substrate was heated up to 400°C in 1×10^{-8} mbar high vacuum and sputter cleaned in pure argon ambient to ensure the removal of any residual organic substance. Then, the silicon nitride (Si_3N_4) film at a constant pressure of 3×10^{-3} mbar and a constant substrate temperature of 200°C was deposited on the substrate using high-purity (99.999%) silicon nitride target.

The ohmic and rectifier contacts were formed using a thermal evaporation system. The ohmic back contacts were formed by the deposition of high-pure Au (99.999%) with a thickness of ~2000 Å at 450°C, under 10^{-7} mbar vacuum and the sample was annealed at 400°C to achieve good ohmic contact behavior. After that, circular dot-shaped rectifier front contacts with 2 mm diameter and ~2000 Å thickness were formed by the deposition of high-purity Au onto Si_3N_4 thin film at 50°C.

The MIS device was irradiated by using a ^{60}Co gamma-ray source with dose rate of 0.69 kGy/h. The MIS device was exposed to various gamma irradiation doses (up to 100 kGy). Both the reverse and forward bias I-V measurements were performed before and after irradiation under dark condition at room temperature by the use of Keithley 2400 source-meter.

3. Results and discussion:

The experimental data is fitted by the conventional thermionic emission (TE) equation. From a fit of the linear region of the forward bias semilogarithmic current-voltage (I-V) curve (V>3kT/q), the values of the electrical parameters are determined [2,16]. The TE equation is given by the following equation:

$$I = I_o \exp\left(\frac{q(V-IR_s)}{nkT}\right)\left[1-\exp\left(-\frac{q(V-IR_s)}{kT}\right)\right] \qquad (1)$$

where I_o is the saturation current, n is the ideality factor, R_s is the series resistance including semiconductor bulk and contact resistance and IR_s term is the voltage drop across the series resistance of device. Due to the existence of series resistance (R_s), a significant voltage drop occurs at large forward currents. In this case, the ln(I)-V curves deviate from a straight line at high forward bias voltage. The slope and intercept of the I-V curve provide ideality factor and saturation current respectively. Saturation current obtained from the straight line intercept of the ln(I) axis at V=0 is given by,

$$I_o = AA^*T^2\exp\left(-\frac{q\Phi_{B0}}{kT}\right) \qquad (2)$$

where A is the contact area, A* is the effective Richardson constant of 112 $Acm^{-2}K^{-2}$ for n-type Si [2] and Φ_{B0} is the zero-bias barrier height. Φ_{B0} is determined using Eq.(2). The ideality factor is a measure of the conformity of diode current to be pure TE. From the slope of ln(I) vs. V curve, the value of n is calculated using the relation:

$$n = \frac{q}{kT}\frac{d(V-IR_s)}{d(\ln I)} \qquad (3)$$

Fig. 1 shows the semi-logarithmic current-voltage (I-V) characteristics of the MIS device as a function of irradiation dose. As seen in Fig. 1(a), the semi-logarithmic forward bias I-V characteristics in the applied bias voltage range of 0.07-0.4 V has a good linear behavior. In this linear range, the series resistance is not effective. On the other hand, after at about 0.42 V, these curves are deviated from linearity especially because of the effect of series resistance and interface states [16-18]. Also, from Fig. 1(a), it is noted that the value of reverse and forward current decreases with the increasing radiation dose.

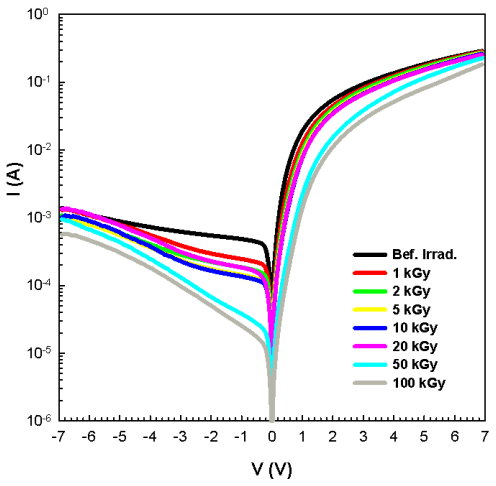

Fig.1: The semi-logarithmic I-V characteristics of Au/Si_3N_4/n-Si (MIS) device before and after irradiation.

The reason for this may be due to the decrease in the generation of carriers as a result of the radiation induced lattice defects and the increase value of series resistance with the increasing radiation dose.

The electrical parameters obtained from forward bias I-V characteristics before and after irradiation are given in Table 1. As shown in Table 1, the value of the ideality factor decreases with the increasing irradiation dose, while the barrier height increases. The decrease in the n could be due to the reduction in carrier density in the depletion region of MIS device through the occurrence of traps and recombination centers associated with radiation damage [19,20]. The higher value of the n, compare to ideal value of 1, is attributed to the interface states, inhomogenities of barrier height, generation-recombination currents and series resistance [1,2,21-24].

Fig. 2 shows a plot of the experimental Φ_{B0} versus n. As seen in Fig. 2, there is a linear relationship between the experimental effective barrier heights and ideality factors of the MIS device. This result can be explained by lateral inhomogeneities of the barrier heights [17,24-28]. The extrapolation of barrier height versus ideality factors to n=1 has given the value of 0.90 eV.

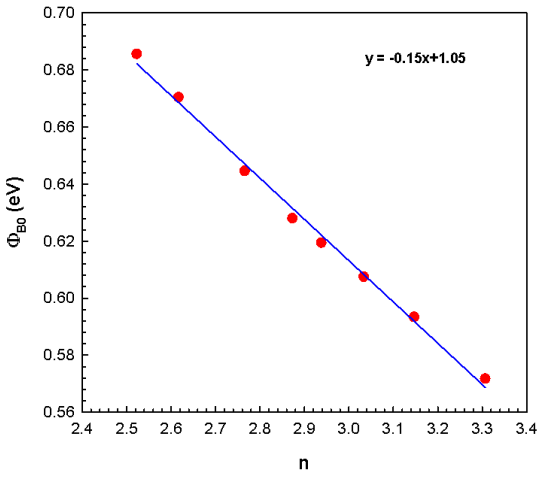

Fig.2: Linear variation of the experimental barrier heights versus ideality factors.

The parasitic resistances such as series resistance (R_s) and shunt resistance (R_{sh}) affect the current-voltage characteristics. The resistance of the device can be expressed as,

$$R_i = \frac{dV_i}{dI_i} \tag{4}$$

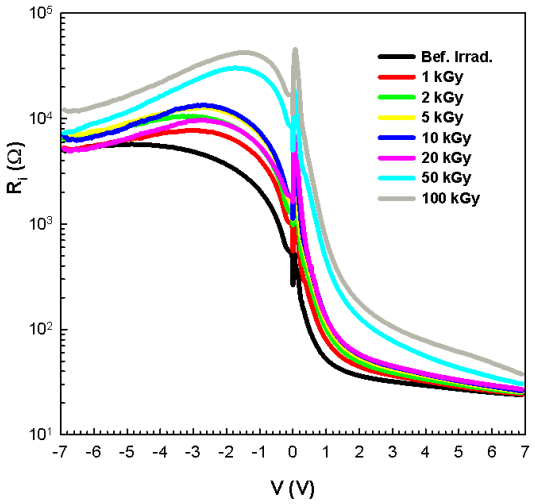

Fig.3: Plots of R_i versus V of the MIS device before and after irradiation dose.

The voltage dependent resistance profile of the MIS device was obtained from the I-V data using Eq. 4 and is given in Fig. 1(b). As seen in Fig. 1(b), at sufficiently high forward bias region (about 7V), the value of resistance corresponds to the R_s for the device. On the other hand, the value of resistance at negative bias region (about -7V) corresponds to the R_{sh} of the device. The values of R_s and R_{sh} in before irradiation and 100 kGy were found to be ~25 Ω and 5 kΩ, and ~40 Ω and 42 kΩ, respectively. It was observed that the values of R_s and R_{sh} are increased with the increasing radiation dose. As a result, the ideal semiconductor devices require the lower R_s and higher R_{sh} [28-30].

The forward bias lnI-V curve deviates from the linearity because of the effect of series resistance (R_s). The value of R_s was calculated using Cheung's method [31]. Cheung's functions are given by the following equations,

$$\frac{dV}{d(\ln I)} = IR_s + n\left(\frac{kT}{q}\right) \tag{5}$$

and

$$H(I) = V - n\left(\frac{kT}{q}\right)\ln\left(\frac{I}{AA^*T^2}\right) = n\Phi_{Bo} + IR_s \tag{6}$$

Eq. (5) and Eq. (6) give straight lines for monotonic regions of the forward bias I-V characteristics (Figs. 3(a) and (b)). In Figs. 3(a) and (b), experimental

dV/dln(I) vs. I and H(I) vs. I plots were presented in before and after gamma-ray irradiation, respectively.

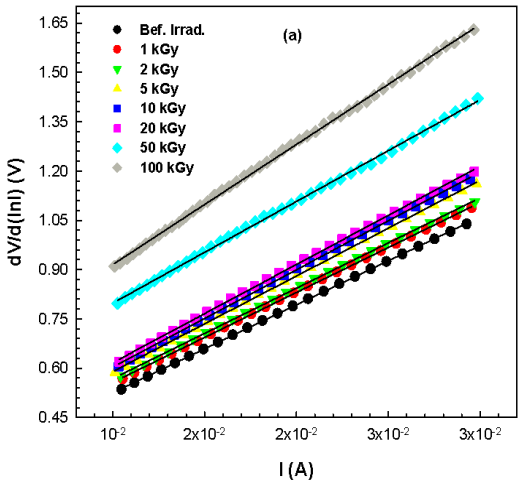

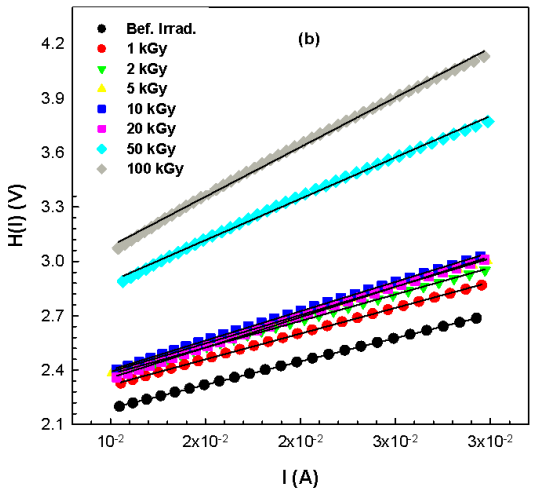

The values of R_s were obtained from the slope of the dV/dln(I) vs. I and H(I) vs. I plots. The calculated values of R_s are shown in Table 1. As shown in Table 1, the values of R_s obtained from both dV/dln(I)-I and H(I)-I plots increase with the increasing irradiation dose.

Such behavior of the R_s can be explained as being due to changes in the effective dopant density due to carrier removal by the defects produced [32-37]. As a result, the obtained R_s values using Cheung's functions are in good agreement with each other.

Conclusions

The effects of gamma ray radiation on the current-voltage (**I-V**) characteristics of Au/Si_3N_4/n-Si (MIS) device have been studied in this paper. The results demonstrate that the electrical parameters of the MIS device obtained from forward bias I-V characteristics are very sensitive to radiation. Experimental results show that while the value of reverse and forward current decreases with the increasing radiation dose, the value of R_s and R_{sh} increases. Furthermore, while the calculated value of n decreases, the Φ_{B0} increases with the increasing gamma irradiation dose. The decrease of the current and ideality factor may be due to creation of radiation-induced interfacial, lattice defects and series resistance. The experimental results indicate that gamma-rays affect the electrical parameters of the MIS device.

Table 1: The electrical parameters obtained from forward bias I-V characteristics.

Irrad. Dose (kGy)	**I_o (A)**	***n***	***Φ_{B0} (eV)***	***R_s dV/d(lnI)) (Ω)***	***R_s (H(I)) (Ω)***
Bef. Irrad.	8.01×10^{-5}	3.31	0.57	26.77	25.79
1	3.47×10^{-5}	3.15	0.59	27.35	28.35
2	2.02×10^{-5}	3.03	0.61	27.51	29.32
5	1.27×10^{-5}	2.94	0.62	29.09	31.28
10	9.12×10^{-6}	2.87	0.63	29.66	32.40
20	4.80×10^{-6}	2.77	0.64	29.90	33.49
50	1.77×10^{-6}	2.62	0.67	30.93	45.65
100	9.84×10^{-7}	2.52	0.69	36.55	51.72

References:

[1] E.H. Nicollian, J.R. Brews, MOS Physics and Technology, Wiley, New York, 1982.
[2] S.M. Sze, K.K. Ng, Physics of Semiconductor Devices, 3rd Ed., John Wiley & Sons, New Jersey, 2007.
[3] H. Bentarzi, Transport in Metal-Oxide-Semiconductor Structures, Springer, New York, 2011.
[4] R. Ertuğrul, A. Tataroğlu, Rad. Eff. Def. Solids 169 (2014) 791.
[5] Ş. Kaya, E. Yılmaz, A. Kahraman, H. Karacali, Nucl. Instr. Meth. B 358 (2015).
[6] L.J. Brillson, C.F. Brucker, A.D. Katnani, N.G. Stoffel, R. Daniels, G. Margaritondo, Surface Science 132 (1983) 212.
[7] A. Kaya, Ş. Altındal, Y.Ş. Asar, Z. Sönmez, Chin. Phys. Lett. 30 (2013) 017301.
[8] A. Tataroğlu, Ş. Altındal, Nucl. Instr. Meth. B 252 (2006) 257.
[9] T.P. Ma, P.V. Dressendorfer, Ionizing Radiation Effect in MOS Devices and Circuits, Wiley, New York, 1989.
[10] T.R. Oldham, Ionizing Radiation Effects in MOS Oxides, World Scientific Publishing, Singapore, 1999.
[11] V.S. Vavilov, Effects of Radiation on Semiconductors, Consultants Bureau, New York, 1965.
[12] A. Johnston, Reliability and Radiation Effects in Compound Semiconductors, World Scientific Publishing, Singapore, 2010.
[13] T.P. Ma, Semicond. Sci. Technol. 4 (1989) 1061.
[14] J.R. Srour, C.J. Marshall, P.W. Marshall, IEEE Trans. Nucl. Sci. 50 (2003) 653.
[15] T.R. Oldham, F.B. McLean, IEEE Trans. Nucl. Sci. 50 (2003) 483.
[16] E.H. Rhoderick, R.H. Williams, Metal-Semiconductor Contacts, 2nd Ed., Clarendon Press, Oxford, 1988.
[17] R.T. Tung, Phys. Rev. B 64 (2001) 205310.
[18] E.H. Nicollian, A. Goetzberger, Appl. Phys. Lett. 7 (1965) 216.
[19] H. Ohyama, J. Vanhellemont, Y. Takami, T. Kudou, H. Sunaga, Rad. Phys. Chem. 53 (1998) 597.
[20] S. Kumar, Y.S. Katharria, D. Kanjilal, J. Phys. D: Appl. Phys. 41 (2008) 105105.
[21] I. Tascıoğlu, A. Tataroğlu, A. Ozbay, Ş. Altındal, Rad. Phys. Chem. 79 (2010) 457.
[22] I. Dokme, Ş. Altındal, I. Uslu, J. Appl. Poly. Sci. 125 (2012) 1185.
[23] O.Y. Olikh, IEEE Trans. Nucl. Sci. 60 (2013) 394.
[24] Ş. Karataş, A. Türüt, Ş. Altındal, Nucl. Instr. Meth. A 555 (2005) 260.
[25] R.F. Schmitsdorf, T.U.Kampen, W. Mönch, J. Vac. Sci.Technol. B 15 (1997) 1221.
[26] S. Aydogan, A. Türüt, Rad. Phys. Chem. 80 (2011) 869.
[27] M. Gokcen, A. Tataroğlu, Ş. Altındal, M.M. Bülbül, Rad. Phys. Chem. 77 (2008) 74.
[28] D. Donoval, M. Barus, M. Zdimal, Solid-State Electron. 34 (1991) 1365.
[29] K.S. Karimov, M.M. Ahmed, S.A. Moiz, M.I. Federov, Sol. Energy Mater. Sol. Cells 87 (2005) 61.
[30] A. Tataroğlu, A.A. Hendi, R.H. Alorainy, F. Yakuphanoğlu, Chin. Phys. B 23 (2014) 057504.
[31] S.K. Cheung, N.W. Cheung, Appl. Phys. Lett. 49 (1986) 85.
[32] A. Rao, S. Krishnan, G. Sajeev, K. Siddappa, Pramana-J. Phys. 74 (2010) 995.
[33] M.Y. Feteha, M. Soliman, N.G. Gomaa, M. Ashry, Renew. Energy 26 (2002) 113.
[34] S. Kar, K.M. Panchal, S. Bhattacharya, S. Varma, IEEE Trans. Electron Dev. 29 (1982) 1839.
[35] S. Alialy, S. Altındal, E.E. Tanrıkulu, D.E. Yıldız, J. Appl. Phys. 116 (2014) 083709 (9 pp).
[36] R.D. Harris, A.J. Frasca, IEEE Trans. Nucl. Sci. 53 (2006) 1995.
[37] A. Tataroğlu, Ş. Altındal, M.M. Bülbül, Nucl. Instr. Meth. A 568 (2006) 863.